

Chemical Synthesis and Characterization Study of Nanocrystalline and Coral Rock-Like Kasterite $\text{Cu}_2\text{ZnSnS}_4$ (CZTS) Thin Films

Sandesh B. Jirage^{1,*}, Kishor V. Gaikwad², Prakash N. Chavan³, Sadashiv A. Kamble³, Vijaykumar Bhuse^{1,*}

* sandeshjirage01@gmail.com, vijaykbhuse13@gmail.com

¹ Thin Film Research Laboratory, Dept. of Chemistry, Government Rajaram College, Kolhapur, 416004, India

² Department of Chemistry, Rajarshi Chhatrapati Shahu College Kolhapur

³ Department of Chemistry, Karmaveer Bhaurao Patil College, Urun Islampur, Dist- Sangli

Received: December 2023

Revised: March 2024

Accepted: March 2024

DOI: 10.22068/ijmse.3540

Abstract: The $\text{Cu}_2\text{ZnSnS}_4$ (CZTS) thin film is a newly emerging semiconductor material in the thin film solar cell industry. The CZTS is composed of economical, common earth-abundant elements. It has advantageous properties like a high absorption coefficient and the best band gap. Here we have applied a low-cost chemical bath deposition technique for the synthesis of CZTS at low temperature, acidic medium and its characterization. The films were characterized by different techniques like X-ray diffraction, Raman, SEM, Optical absorbance, electrical conductivity and PEC study. The X-ray diffraction and Raman scattering techniques were utilized for structural study. The XRD reveals the kasterite phase and nanocrystalline nature of CZTS thin films. These results and their purity were confirmed further by advanced Raman spectroscopy with a 335 cm^{-1} major peak. The crystallite size was found to be 50.19 nm. The optical absorbance study carried out by use of UV-visible spectroscopy analyses its band gap near about 1.5 eV and its direct type of absorption. The electrical conductivity technique gives a p-type of conductivity. The scanning electron microscopy (SEM) study finds its rock-like unique morphology. The EDS technique confirms its elemental composition and its fair stoichiometry. The analysis of PEC data revealed power conversion efficiency-PCE to 0.90%.

Keywords: Nanocrystalline, Semiconductor, Solar cells, Thin films, CZTS.

1. INTRODUCTION

The whole world has been troubled by complicated environmental issues due to the enormous utilization of fossil fuels. To overcome increasing energy crises, solar energy is a more renewable option than any other limited resource. The solar energy is based on photovoltaic technology. The recent PV technology of thin film solar cells has excessively used silicon, cadmium telluride (CdTe) and copper indium gallium diselenide (CIGS) as semiconductor materials. But these materials have severe limitations like high processing costs of silicon, composition of rare earth elements like In, Ga and toxicity of elements like Cadmium (Cd) [1, 2]. Hence these materials will not be helpful in future to satisfy ever-increasing energy requirements with a green environment approach.

The current PV technology needs semiconductor materials whose elements have a plentiful composition in the earth's crust which is helpful in the fabrication of low-cost and environmentally benign solar cells. In this regard, $\text{Cu}_2\text{ZnSnS}_4$ (CZTS) has been explored extensively as the

environment's best promising absorber materials due to their excellent optoelectronic properties like band gap 1.5 eV and having as high as absorption coefficient over 10^4 cm^{-1} [3-4]. The CZTS is a p-type semiconductor material with a composition of ample and harmless elements. The CZTS has two primary structures kasterite and stannite type which have diverse arrangements of Cu^{1+} and Zn^{2+} atoms in the crystal structure [5]. However, Kasterite CZTS is thermodynamically more stable [6]. Overall CZTS is a substitute absorber material for the existing scenario of semiconductor material.

So far CZTS thin films have been prepared by several techniques such as RF magnetron sputtering deposition [7], thermal evaporation [8], atom electron-beam-evaporation [9], pulsed laser deposition [10], etc. but these vacuum methods are costlier due to its special requirements and high-temperature processes. Other non-vacuum methods involve sol-gel deposition [11], spray pyrolysis [12], chemical vapor deposition [13], spin coating technique [14], electrodeposition methods [15], nanoparticle methods [16], silar method [17] etc. To date, the solar cell based on

pure CZTS has achieved power conversion efficiency as high as 9.2% [18]. Hence there is a need for improvement. The chemical bath deposition method (CBD) has attracted wide attention from researchers because of its simple, economical equipment and low-temperature processes [19]. In this work, we report on the synthesis of CZTS using the CBD method in an acidic medium and its characterization which resulted from nanocrystalline, kasterite CZTS thin films having typical rock-like morphology. The films were characterized by X-ray diffraction, Raman spectroscopy, optical absorbance, electrical conductivity, scanning electron microscopy, and EDS techniques.

2. EXPERIMENTAL PROCEDURES

The chemicals used like copper sulphate [Cu(SO₄).5H₂O], zinc sulphate (ZnSO₄.H₂O), stannic chloride (SnCl₄.5H₂O), Thiourea and tartaric acid solution, etc. were of analytical grade (A. R) (Sigma Aldrich). The films were deposited on commercially available, non-conducting micro-glass slides (Blue Star, India) having dimensions of 75 x 25 x 1.35 mm. The slides were cleaned by washing with chromic acid for about thirty minutes followed by rinsing in acetone, distilled water and then used for deposit.

The 10 ml CuSO₄ solution, 5 ml ZnSO₄, and 5 ml SnCl₄ (each of 0.2 M) were taken in 250 mL beaker, followed by drop-wise addition of complexing agent tartaric acid (0.2 M and 40 mL) and then the addition of 20 mL thiourea solution (0.2 M) as sulphur source slowly at room temperature. The solution was stirred well for about 15 minutes. The final volume was maintained to 200 mL by using double distilled water. The pH of the reactive mixture was adjusted to 5.5 (acidic). The beaker was then kept on heating the magnetic stirrer. The clean glass slides are vertically positioned properly by the substrate holder. The speed of the magnetic stirrer in the reaction mixture was maintained at 40 rpm. The temperature of the reaction bath was then allowed to increase slowly and slowly. When the temperature reached 50°C which was kept constant for 180 minutes. The parameters like pH, temperature and duration of deposition time were optimized by carrying out repetition of the deposition process to achieve the best quality of films. The slides were removed, washed with

distilled water very carefully and were subjected to drying in nature at room temperature. Then films were air annealed at 200°C as per requirement. The CZTS films appear to be white. The schematic diagram of the set-up of the CBD method is represented in Fig. 1.

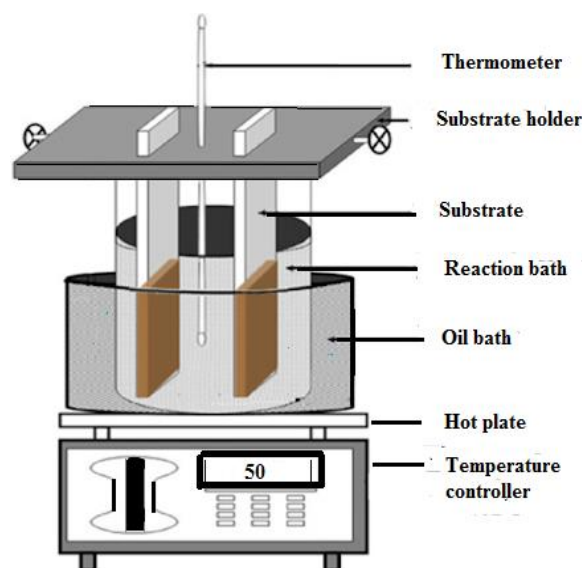


Fig. 1. \ Set up of CBD method.

2.1. Characterization Techniques

The XRD study of the CZTS thin film was carried out in the diffraction angle (2θ) range of 10-80° with CuK α 1 ($\lambda = 1.54056 \text{ \AA}$) radiation by using a Philips PW-1710 diffractometer. The Raman spectrum was recorded by the HORIBA JobinYvon Raman micrometre at room temperature. The operating excitation wavelength of 532 nm and laser power of 15 mV were used. The 'dc' four probes (equal spacing) method was used to measure the electrical conductivity of the CZTS thin film. The optical absorption measurements were made in the wavelength ranging from 400 to 1100 nm by using a UV 3600 Shimadzu UV-VIS-NIR double beam spectrophotometer at room temperature. The study of surface morphology was done by Scanning electron microscopy (SEM) JEOL-mode-JSM -6390-SEM associated with Energy dispersive spectrometry (EDS) for elemental composition. The PEC properties were measured on Keithley Model-4200 (SCS).

3. RESULTS AND DISCUSSION

3.1. Structural Characterization

The XRD patterns of the annealed CZTS thin film at 200°C in the air (for 1 h) are shown in Fig. 2.

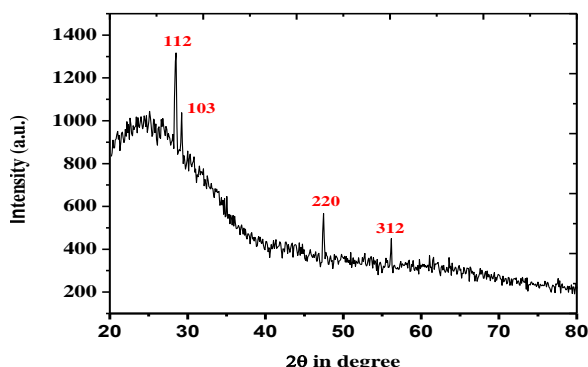


Fig. 2. X-ray diffraction patterns of annealed CZTS thin films.

The sharp peaks of CZTS thin film at the 2θ angles: 28.50, 29.31, 47.40 and 56.14 which corresponds to (112), (103), (220) and (312) orientations exactly match JCPDS card number 26-0575 for CZTS. The main diffraction peaks are indexed to (112) point out CZTS film with Kasterite structure [20]. The major peaks in annealed film also indicate a nanocrystalline form of CZTS. The XRD is not lonely sufficient to confirm CZTS, because of its close XRD pattern like ZnS and Cu_2SnS_3 . The 112 peaks of kasterite CZTS are very close to the 111 peaks of cubic ZnS. But here CZTS have shown an additional peak at 2θ , 29.31 of (103) plane which surely points out the formation of CZTS [21]. The crystallite size (D) of CZTS calculated by Debye-Scherrer's formula is represented below.

$$D = 0.9\lambda / \beta \cos \theta \quad (1)$$

Where D-crystallite size, λ -Wavelength of X-ray (Å), β -FWHM intensity in radian, θ -Bragg's diffraction angle. The crystallite size for a more intense peak was used hence peak of (112) peak of CZTS using its Full Width Half Maximum (FWHM) the crystallite size which was found to be 50.19 nm. This also strongly approved that CZTS film is composed of nanocrystals. The interplane spacing (d) values calculated by Bragg's law which were found to be 3.1164,

2.7150, 1.9104, and 1.5722 (Å) for 112, 103, 220, 312 planes respectively were close to reported standard data. Table 1 describes the comparison of 2θ and d values compared with standard values of CZTS thin film. Besides X-ray analysis, the Raman spectrum was recorded by using Raman spectroscopy measurements. Fig. 3 shows RAMAN peaks of the annealed CZTS thin film at 200°C in the air (for 1 h). The Raman spectrum gives evidence of peaks at 335 cm^{-1} as a major peak along with 286 cm^{-1} and 367 cm^{-1} which are attributed to the pure kasterite CZTS [22].

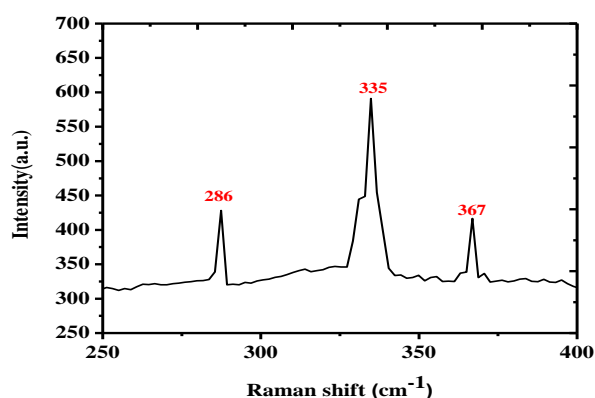


Fig. 3. Raman spectrum of annealed CZTS thin films.

3.2. Morphological and Compositional Analysis

Scanning electron microscopy (SEM) is the most useful technique for the study and examination of surface morphology thin films. The SEM of the annealed CZTS thin film is shown in Fig. 4 under different magnifications. The surface morphology exhibited by the annealed CZTS thin film (200°C) is coral-rock with an almost uniform texture and larger in thickness (Fig. 2) without any cracks and voids in the absorber.

The homogeneous distribution of the CZTS through the film is seen. This typical coral rock-like morphology is helpful to increase the efficiency of solar cells [23]. The crystal size from the SEM photograph though seems to be larger in comparison to XRD.

Table 1. Comparison of 2θ and d values with standard values.

Standard d values (Å)	Observed d values (Å)	Standard 2θ values (°)	Observed 2θ values (°)	Plane
3.126	3.1164	28.53	28.50	112
3.008	2.7150	29.67	29.31	103
1.919	1.9104	47.32	47.40	220
1.565	1.5722	58.96	57.22	312

As per the study, such discrepancies may be observed due to the possibility of elemental loss during annealing at higher temperatures. The elemental composition of CZTS thin film was determined by using Energy dispersive X-ray analysis (EDS).

Its atomic mass percentage was found to be Cu= 22.86%, Zn= 13.44%, Sn= 13.03% and S= 50.67% which confirms that Cu:Zn:Sn:S elements are consistent in their 2:1:1:4 stoichiometry. The EDS also reveals CZTS thin film Cu rich and Zinc poor. The EDS spectrum is shown in Figure 5.

3.3. Optical Properties of CZTS

The optical absorption study is recorded on a double-beam spectrophotometer at the wavelength range of 400 to 1100 nm. Figure 6a shows the optical absorption spectrum of the annealed CZTS thin film which is used to calculate band gap energy.

The variation of the absorption coefficient function with wavelength is also shown in Figure 6b. The band gap of a material obeys the relation near the absorption edge, which is according to S. Mushtaq et al. [24].

$$\alpha h\nu = B(h\nu - E_g)^x \quad (2)$$

Where B- constant, $h\nu$ - wavelength of the light used, E_g - band gap of the material and x are factors that depend on the kind of transitions involved. The extrapolation of a linear portion of the graph gives a direct band gap (E_g) of 1.5eV at room temperature. The value of the band gap of CBD-deposited CZTS is a good agreement with the reported value (1.5 eV) and is applicable for solar cells [8-9].

3.4. Electrical Conductivity and Photoelectrochemical (PEC) Measurement

The type of conductivity of a film material can be determined by the electrical resistivity of the material which follows the Arrhenius relation and it is temperature reliance.

$$\rho = \rho_0 \exp(-E_a/kT) \quad (3)$$

Where E_a - activation energy, k- Boltzmann constant, T- absolute temperature, and ' ρ ' and ' ρ_0 ' are the resistivity and specific resistivity respectively. The measurement of electrical resistance of CZTS thin films was completed at ranging from room temperature to 150°C. The variation of the log ' ρ ' vs. inverse absolute temperature is exhibited in Fig. 7.

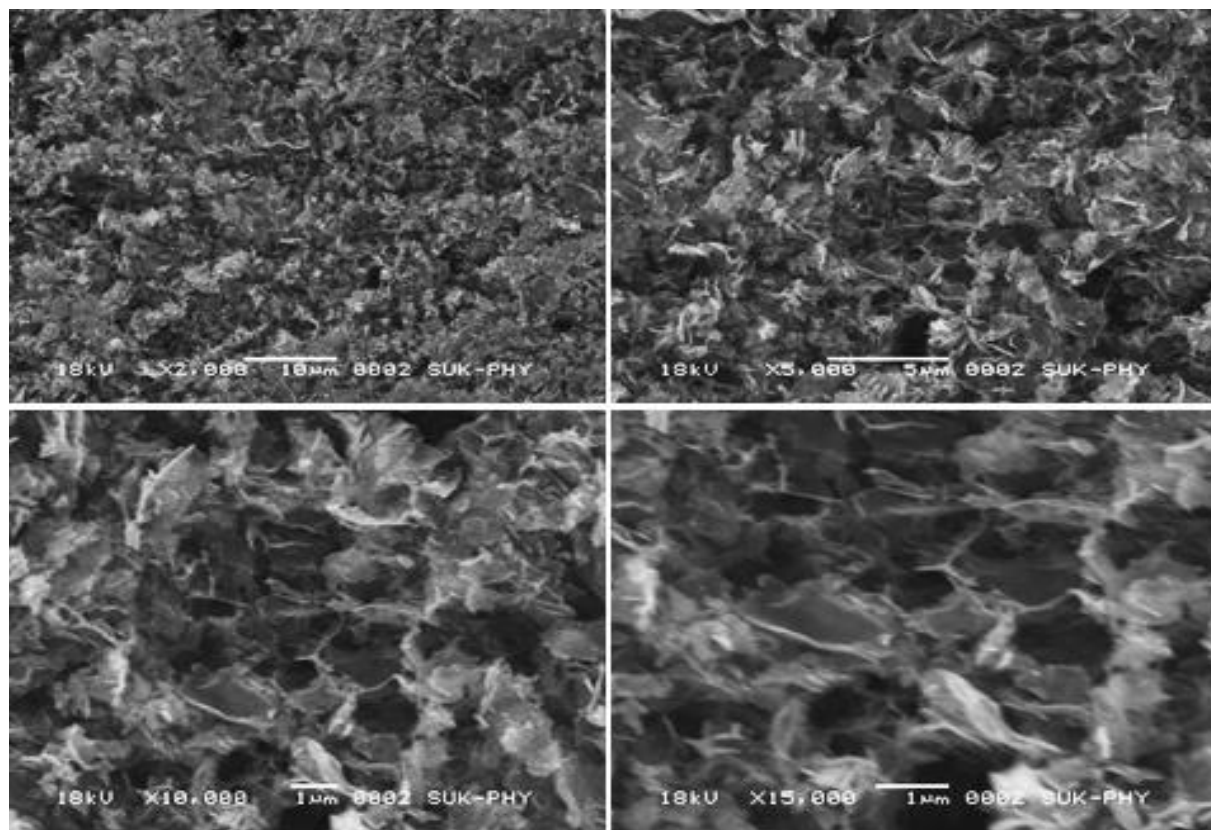


Fig. 4. SEM of coral-rock-like morphology of CZTS.

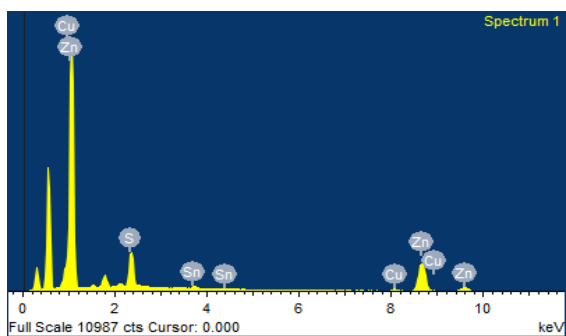


Fig. 5. EDS spectrum of annealed CZTS films.

The nature of the plot is linear which confidently showed that the presence of only one type of conduction mechanism. The resistivity decreases with temperature increases. The activation energy of the CZTS film calculated from the above plot was found to be 0.648 eV. The electrical properties of CBD-deposited CZTS agree with the requirements for potential applications in thin film solar cell invention [25].

The PEC performance of CZTS film was studied by depositing on conducting Fluorine doped Titanium Oxide (FTO) coated glass substrate. The films were annealed at 200°C to remove impurity phases if any and we observed good results by XRD & Raman study of CZTS thin films annealed at 200°C which was mentioned in structural analysis. Its PEC analysis was done under illumination.

The CZTS worked as a photoelectrode, whose 1 cm³ unmasked surface and graphite rod as a counter electrode were utilized. The iodine redox solution in NaOH (both 0.1 M) solution was used as an electrolyte. The distance between the two electrodes was kept at least 3 mm. Figure 8 shows the variation of the current density-voltage curve of CZTS thin films at room temperature. The power conversion efficiency (η) can be calculated

by the following relation as the power input is known (i.e. 30 mW).

$$\eta = \frac{\text{Power output}}{\text{Input power}} = \frac{V_m \cdot I_m}{\text{Input power}} \quad (4)$$

The analysis of PEC data revealed a stable power conversion efficiency (η) of 0.90%. The data was calculated from an open circuit voltage (V_{oc}) of 470 mV, a short circuit current (I_{sc}) of 12.0 mA/cm² and a fill factor is 0.48 of a CZTS film [26]. Recently fill factor of 32.78% was reported with 1.01% efficiency for CZTS thin film by Vu Minh Han Cao *et.al* [27].

4. CONCLUSIONS

It is a low-cost chemical bath deposition method that results in kasterite and nanocrystalline CZTS thin films. The very recordable thing was the acidic medium used to synthesise CZTS by using a non-toxic tartaric acid complex. The structural study and kasterite phase with purity of CZTS were analyzed by XRD. The result of XRD and purity of CZTS were further confirmed by the RAMAN study. A SEM study exhibits unique coral rock-like morphology. The CZTS film exhibits a good stoichiometry, high absorption coefficient, and direct band gap of 1.5 eV optimum and ideal for solar absorption. The conductivity measurement showed a single type of conduction. The PEC study reveals a stable power conversion efficiency of 0.90%. Overall CZTS was deposited at a very low temperature and economical CBD method.

ACKNOWLEDGEMENTS

The authors SBJ and VMB are grateful to Shivaji University, Kolhapur, India for authorization to carry out the research work.

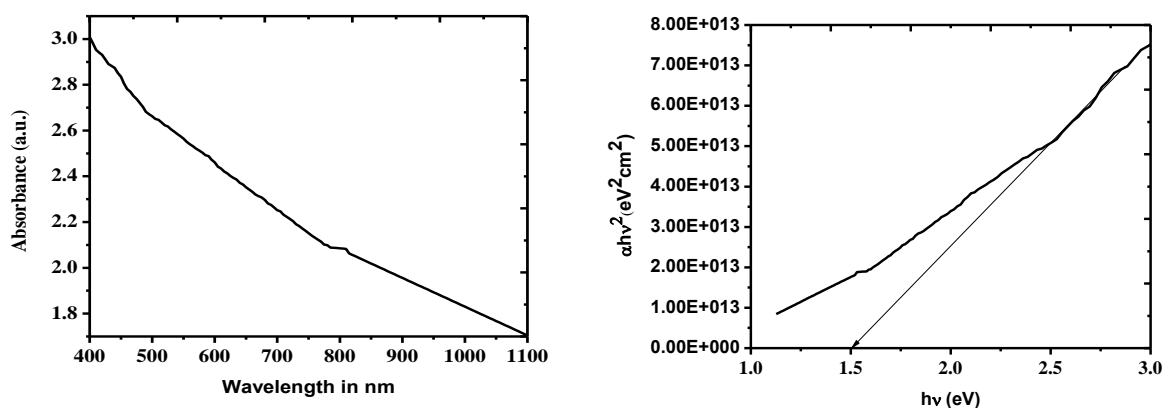


Fig. 6. a) Optical absorption spectrum of CZTS thin film; b) Plot of $(\alpha h\nu)^2$ vs $h\nu$ of CZTS thin films.

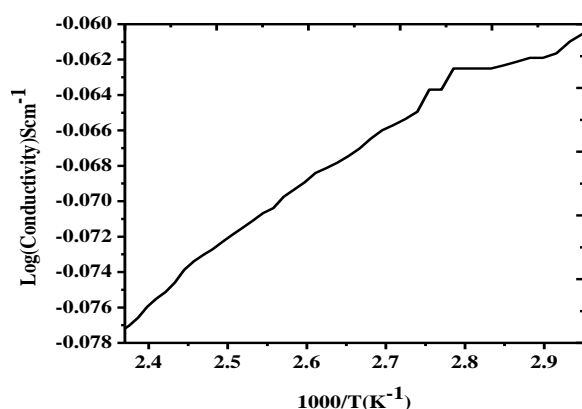


Fig. 7. Plot of log conductivity vs. inverse absolute temperature.

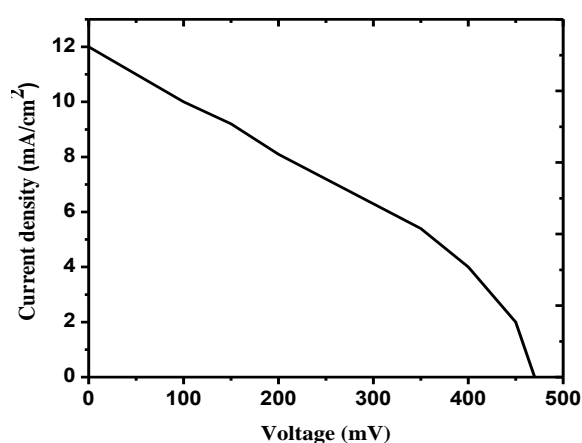


Fig. 8. Current-voltage (I-V) characteristics of CZTS thin films.

REFERENCES

- [1] Afrina Sharmin, M. S. Bashar, Munira Sultana, and S. M. Mostafa Al Mamun, Sputtered single-phase kesterite $\text{Cu}_2\text{ZnSnS}_4$ (CZTS) thin film for photovoltaic applications: Post annealing parameter optimization and property analysis. *AIP Advances*, 2020, 10, 015230.
- [2] A. Wangperawong, J.S. King, S.M. Herron, B.P. Tran, K. Pangan-Okimoto, S.F. Bent, Aqueous bath process for deposition of $\text{Cu}_2\text{ZnSnS}_4$ photovoltaic absorbers. *Thin Solid Films*, 2011, 519, 2488-2492.
- [3] Sandip Mahajan, Elias Stathatos, Nanasheb Huse, Ravikiran Birajdar, Alexandros Kalarakis, Ramphal Sharma, Low-cost nanostructure kesterite CZTS thin films for solar cells application. *Materials Letters* 2018, 210, 92–96.
- [4] Andigoni Apostolopoulou, Sandip Mahajan, Ramphal Sharma, Elias Stathatos, Novel development of nanocrystalline kesterite $\text{Cu}_2\text{ZnSnS}_4$ thin film with high photocatalytic activity under visible light illumination. *Journal of Physics and Chemistry of Solids* 2018, 112, 37–42.
- [5] S. Y. Chen, X. G. Gong, A. Walsh and S. H. Wei, Crystal and electronic band structure of $\text{Cu}_2\text{ZnSnX}_4$ (X= S and Se) photovoltaic absorbers: First-principles insights. *Appl. Phys.Lett.*, 2009, 94, 041903.
- [6] S. Schorr, Structural aspects of adamantine like multinary chalcogenides. *Structural aspects of adamantine like multinary chalcogenides. Thin Solid Films*, 2007, 515(15), 5985-5991.
- [7] M.A. Olgar, J. Klaer, R.Mainz, L.Ozyuzer, T. Unold, $\text{Cu}_2\text{ZnSnS}_4$ -based thin films and solar cells by rapid thermal annealing processing. *Thin Solid Films* 2017, 628, 1-6.
- [8] B. Shin, Y. Zhu, T. Gershon, N.A. Bojarczuk, S. Guha, Epitaxial growth of kesterite $\text{Cu}_2\text{ZnSnS}_4$ on a Si (001) substrate by thermal co-evaporation. *Thin Solid Films*, 2014, 556, 9-12
- [9] H. Katagiri, K. Saitoh, T. Washio, H. Shinohara, T. Kurumadani, S. Miyajima, Synthesis and characterization of $\text{Cu}_2\text{ZnSnS}_4$ thin films by SILAR method. *Sol. Energy Mater. Sol. Cells* 2001, 65, 14-148.
- [10] A.V. Vanalakar, S.W. Shin, G. L. Agawane, M. P. Suryawanshi, K. V. Gurav, P.S. Patil, and J.H. Kim, A review on pulsed laser deposited CZTS thin films for solar cell applications. *Journal of Alloys and Compounds* 2015, 619, 109–121.
- [11] L. Dong, S. Cheng, Y. Lai, H. Zhang, H. Jia, Sol-gel processed CZTS thin film solar cell on flexible molybdenum foil. *Thin Solid Films* 2017, 626, 168–172.
- [12] S.A. Khalate, R.S. Kate, J.H. Kim, S.M. Pawar, R.J. Deokate Effect of deposition temperature on the properties of $\text{Cu}_2\text{ZnSnS}_4$ (CZTS) thin films. *Superlattices and Microstructures* 2017, 103, 335e342.
- [13] T. Washio, T. Shinji, S. Tajima, T. Fukano, T. Motohiro, K. Jimbo and H. Katagiri, 6% Efficiency $\text{Cu}_2\text{ZnSnS}_4$ -based thin film solar cells using oxide precursors by open

- atmosphere type CVD. *J. Mater. Chem.*, 2012, 22, 4021.
- [14] K. Liu, B. Yao, Y. Li, Z. Ding, H. Sun, Y. Jiang, G. Wang and D. Pan, A versatile strategy for fabricating various $\text{Cu}_2\text{ZnSnS}_4$ precursor solutions. *J. Mater. Chem. C*, 2017, 5, 3035-3041.
- [15] K.V. Gurav, S.M. Pawar, S. W. Shin, M.P. Suryawanshi, G.L. Agawane, P.S. Patil, J.H. Moon, J.H. Yun, and J.H. Kim, Electrosynthesis of CZTS films by sulfurization of CZT precursor: Effect of soft annealing treatment. *Applied Surface Science* 2013, 283, 74– 80.
- [16] M.P. Suryawanshi, S. W. Shin, U. Ghorpade, D. Song, C. W. Hong, S. Han, J. Heo, S. H. Kang and J. H. Kim, A facile and green synthesis of colloidal $\text{Cu}_2\text{ZnSnS}_4$ nanocrystals and their application in highly efficient solar water splitting. *J. Mater. Chem. A*, 2017, 5, 4695.
- [17] M.P. Suryawanshi, S.W. Shin, U.V. Ghorpade, K.V. Gurav, C.W. Hong, G.L. Agawane, S.A. Vanalakar, J.H. Moon, J. H. Yun, P.S. Patil, J. H. Kim, A.V. Moholkar, Improved photoelectrochemical performance of $\text{Cu}_2\text{ZnSnS}_4$ (CZTS) thin films prepared using modified successive ionic layer adsorption and reaction (SILAR) sequence. *Electrochimica Acta* 2014, 150, 136–145.
- [18] T. Kato, H. Hiroi, N. Sakai, S. Muraoka, and H. Sugimoto, Proceedings of the 27th European Photovoltaic Solar Energy Conference, Frankfurt, Germany, 2012, 2236–2239.
- [19] T. R. Rana, N.M. Shinde and J.H. Kim, *Materials Letters.*, (2016) 162, 40-43.
- [20] J. Tao, K. Zhang, C. Zhang, L. Chen, H. Cao, J. Liu, J. Jiang, L. Sun, P. Yang and J. Chu, A sputtered CdS buffer layer for co-electrodeposited $\text{Cu}_2\text{ZnSnS}_4$ solar cells with 6.6% efficiency. *Chem. Commun.*, 2015, 51, 10337–10340.
- [21] Jie Ge, S. Zuo, J. Jiang, Jianhua Ma, L. Yang and J. Chu, Simplest synthesis and characterization study of flower-like $\text{Cu}_2\text{ZnSnS}_4$ thin films. *Applied surface science*, 2012, 258, 7844-48.
- [22] Suryawanshi, M. P., Shin, S. W., Ghorpade, U. V., Gurav, K. V., Agawane, G. L., Hong, C. W., Jae Ho Yun, P. S. Patil, Jin Hyeok Kim, Moholkar, A. V. (2014). A chemical approach for the synthesis of photoelectrochemically active $\text{Cu}_2\text{ZnSnS}_4$ (CZTS) thin films. *Solar Energy*, 2014, 110, 221-230.
- [23] Patil, U. M., Gurav, K. V., Fulari, V. J., Lokhande, C. D., & Joo, O. S. Characterization of honeycomb-like “ β -Ni(OH) $_2$ ” thin films synthesized by chemical bath deposition method and their supercapacitor application. *Journal of Power Sources*, 2009, 188(1), 338-342.
- [24] S. Mushtaq, B. Ismail, M. A. Zeb, N. J. S. Kissinger and A. Zeb, *J. Alloys Compd.*, (2015) 632, 723-728.
- [25] Scragg, J. J., Dale, P. J., Peter, L. M., Zoppi, G., & Forbes, I. New routes to sustainable photovoltaics: evaluation of $\text{Cu}_2\text{ZnSnS}_4$ as an alternative absorber material. *physica status solidi (b)*, 2008, 245(9), 1772-1778.
- [26] Dhakal, T. P., Peng, C. Y., Tobias, R. R., Dasharathy, R., & Westgate, C. R. Characterization of a CZTS thin film solar cell grown by sputtering method. *Solar Energy*, 2014, 100, 23-30.
- [27] Cao, V. M. H., Bae, J., Shim, J., Hong, B., Jee, H., & Lee, J. Fabrication of the $\text{Cu}_2\text{ZnSnS}_4$ thin film solar cell via a photo-sintering technique. *Applied Sciences*, 2021, 12(1), 38.